A genome-scale CRISPR screen identifies the ERBB and mTOR signalling networks as key determinants of response to PI3K inhibition in pancreatic cancer

Charlotte K. Milton[1], Annette J. Self[1], Paul A. Clarke[1], Udai Banerji[1,2], Federica Piccioni[3], David E. Root[3] and Steven R. Whittaker[1†]

[1]Division of Cancer Therapeutics, The Institute of Cancer Research, London, UK.

[2]The Royal Marsden NHS Foundation Trust, London, UK

[3]The Broad Institute, Cambridge, MA 02142, USA.

Running title

ERBB and mTOR drive resistance to PI3K inhibition

[†]Corresponding author

Dr Steven R Whittaker

Division of Cancer Therapeutics

The Institute of Cancer Research

London SW7 3RP

United Kingdom

Tel: +44 208 722 4220

Email: steven.whittaker@icr.ac.uk

Word count: 5473 (Excluding abstract, methods, additional information and references)

Key words

Pancreatic cancer, KRAS, CRISPR, PI3K, resistance.

Additional Information

Conflict of interest

C.K. Milton, A.J. Self, P.A. Clarke, U. Banerji and S.R. Whittaker are employees of the Institute of Cancer Research that has a commercial interest in the development of PI3K inhibitors. P.A. Clarke is a recipient of an ICR awards to inventors payment for the discovery of GDC0941.

Authors' contributions

Conception and design: CKM and SRW

Development of methodology: CKM, FP, DER, SRW

Acquisition of data: CKM, AJS, FP, SRW

Analysis and interpretation of data: CKM, FP, SRW

Writing, review and/or revision of manuscript: CKM, FP, DER, SRW

Administrative, technical, or material support: AJS, FP, DER, SRW

Study supervision: PAC, UB, FP, DER, SRW

Abstract

KRAS-mutation is a key driver of pancreatic cancer and PI3K pathway activity is an additional requirement for *Kras*-induced tumorigenesis. Clinical trials of PI3K pathway inhibitors in pancreatic cancer have shown limited responses. Understanding the molecular basis for this lack of efficacy may direct future treatment strategies with emerging PI3K inhibitors. We sought new therapeutic approaches that synergise with PI3K inhibitors through pooled CRISPR modifier genetic screening and a drug combination screen. ERBB-family receptor tyrosine kinase signalling and mTOR signalling were key modifiers of sensitivity to alpelisib and pictilisib. Inhibition of the ERBB-family or mTOR was synergistic with PI3K inhibition in spheroid, stromal co-cultures. Near-complete loss of ribosomal S6 phosphorylation was associated with synergy. Genetic alterations in the ERBB-PI3K signalling axis were associated with decreased survival of pancreatic cancer patients. Suppression of the PI3K/mTOR axis is potentiated by dual PI3K and ERBB family or mTOR inhibition. Surprisingly, despite the presence of oncogenic KRAS, thought to bestow independence from receptor tyrosine kinase signalling, inhibition of the ERBB family blocks downstream pathway activation and synergizes with PI3K inhibitors. Further exploration of these therapeutic combinations is warranted for the treatment of pancreatic cancer.

Introduction

The 10-year survival rate for pancreatic ductal adenocarcinoma (PDAC) has remained at just 3 % for the past 40 years (1). Activation of the oncogene, *KRAS*, is one of the earliest genetic alterations detected in the development of PDAC and *KRAS* mutations are found in over 90 % of cases (2,3). Transgenic mouse models expressing oncogenic *Kras*^{G12D} have demonstrated that mutant *KRAS* is an important driver in pancreatic cancer, as switching off Kras signalling results in tumour regression (4). Recently discovered inhibitors of KRAS^{12C} have further validated the dependency of pancreatic, colon and lung tumor models on oncogenic KRAS and demonstrated promising early clinical activity (5,6).

There is a strong rationale for targeting PI3K in PDAC. Activation of the PI3K pathway is commonly observed in PDAC patient samples (7-9), regulates cell metabolism, growth and survival and is commonly implicated as a driver of human cancer (10). Importantly, phosphorylation of PI3K signalling markers, including AKT (Ser473), mTOR (Ser2448) and GSK3β (Ser9) (11) or low expression of PTEN, a suppressor of PI3K signalling (12), is predictive of poor survival in pancreatic cancer. Moreover, the interaction between Ras and PI3Kα is essential for Kras^{G12D}-induced tumorigenesis in mice (13). Notably, Kras^{G12D}-driven murine PDAC tumours are dependent on PI3Kα (14,15) but not PI3Kβ (15), or Craf (14) for tumorigenesis. Consequently, PI3K signalling is an attractive therapeutic target for PDAC. However, clinical trials of allosteric mTOR inhibitors, including temsirolimus (7), or everolimus (16), have shown limited activity in gemcitabine-refractory, metastatic pancreatic cancer patients, likely due to loss of negative feedback on IRS1 and reactivation of PI3K (16). Multiple oncogenic pathways are engaged downstream of KRAS (17,18), so it is perhaps unsurprising that targeting a single downstream effector may not be enough to affect cell viability. We hypothesise that PI3K inhibition selects for compensatory mechanisms sufficient to maintain tumour cell survival.

This study aimed to elucidate the mechanisms of intrinsic resistance to PI3K inhibition in pancreatic cancer and identify rational drug combinations to overcome them. Functional genomic screens have successfully identified loss-of-function events that drive drug resistance, finding NF1 loss to be a key driver of resistance to RAF inhibition in melanoma (19). We therefore employed a genome-scale synthetic lethal CRISPR screen to find loss of function events that could modulate sensitivity to PI3K inhibition. We discovered that the ERBB and mTOR signalling networks regulate response to PI3K inhibition in PDAC. Furthermore, we used a combination drug screen to prioritise clinically relevant targeted agents that synergise with PI3K inhibition to improve therapeutic response.

Materials and Methods

Cell lines and cell culture

Pancreatic cancer cell lines were a kind gift from Dr Anguraj Sadanandam (The Institute of Cancer Research), with the exception of PANC1, PATU8902, MIAPACA2, YAPC and HEK293T cells, which were obtained from the American Tissue Culture Collection (ATCC). T47D cells were from the Deutsche Sammlung von Mikroorganismen und Zellkulturen (DSMZ). All cells were cultured in Dulbecco's Modified Eagle Medium (Sigma) supplemented with 10 % Fetal Bovine Serum (FBS Good, Pan Biotech), with the exception of MIAPACA2 which was supplemented with 20 % FBS. Human pancreatic stellate cells (PSC) were obtained from ScienCell laboratories. Recombinant growth factors were obtained from Bio-Techne. Cell lines were tested for mycoplasma using the MycoAlert Mycoplasma Detection Kit (Lonza). Cell line authentication was not performed.

Small molecule inhibitors

All small molecule inhibitors were purchased from Selleck Chemicals: BYL719 (S2814), GDC0941 (S1065), pelitinib (S1392), everolimus (S1120), AZD8055 (S1555), AZD2014 (S2783) and BEZ235 (S1009). Stock solutions were prepared in dimethylsulfoxide (DMSO) and stored at -20°C.

Cell proliferation assays

For GI_{50} determinations, cells were seeded in 96 well plates. The next day, cells were treated with increasing concentrations of inhibitor or with DMSO alone. After a 72 h incubation period, cell proliferation was quantified using CellTiter-Blue reagent (Promega) and normalised to DMSO treated wells. GI_{50} values were calculated using non-linear regression analysis in GraphPad Prism software. For population doubling experiments, cells were seeded at an initial density of $1x10^7$ cells/flask in 225 cm^2 flasks. Cells were allowed to proliferate to 80-90 % confluence before they were counted and then reseeded at the same initial density. Population doublings (PD) were calculated according to the equation below.

$$\textbf{Population doublings} = \frac{\text{Log (cell count/initial cell number)}}{\text{Log (2)}}$$

For determination of maximum excess above bliss, cells were treated with a matrix of increasing concentrations of two inhibitors or DMSO. After a 72 h incubation period, cell proliferation was quantified using CellTiter-Blue reagent and normalised to the DMSO treated well. The Bliss independence model (20) was used to calculate synergy.

For colony assays, cells were seeded in 12 well plates. The next day, triplicate wells were treated with DMSO, the inhibitors alone or the combinations. After 14 d, cells were washed with PBS and fixed in 4 % formaldehyde/PBS for 30 min. Cells were stained with 0.5 % crystal violet in 70 % ethanol and imaged using a FluoroChem E imaging system (Protein Simple). Colonies were quantified by solubilising the crystal violet solution in 10 % acetic acid and reading the absorbance at 595 nm using an EMax® Plus Microplate Reader (Molecular Devices).

Spheroid growth assays

Human pancreatic stellate cells (PSC) were cultured in Dulbecco's Modified Eagle's Medium/Nutrient Mixture F-12 Ham (Sigma Aldrich), supplemented with 1 % GlutaMAX (ThermoFisher Scientific), 1 % Amphotericin B (ThermoFisher Scientific), 1 % Penicillin-Streptomycin (Sigma Aldrich) and 10 % Fetal Bovine Serum (FBS Good, Pan Biotech). Cells were seeded in co-culture with established PDAC cell lines at a starting density of $1x10^3$ cells/well in 96 well Ultra-low Attachment Round Bottom Multi-well Plates (Nexcelom). Cells were seeded to form spheroids at a ratio of 1:1 PSCs to PDAC cell lines. The next day, cells were treated with DMSO, fixed concentrations of drugs or the desired combinations. Spheroid diameter was measured over a time period of 10 d, with measurements taken every 3-4 d. The first measurement was taken the day after cells were plated, before the addition of DMSO and drug treatments. Spheroid diameter was imaged and quantified using the Celigo Imaging Cytometer (Nexcelom) and is the average of at least 3 replicate spheroids. For viability staining, spheroids were incubated with 1 µM calcein AM and 40 µg/ml propidium iodide for 30 min prior to imaging.

Cell lysis and Western blotting

After the desired treatment, cells were washed with cold PBS and lysed in NP40 buffer (0.5 % NP40, 150 mM NaCl, 50 mM Tris pH7.5, Pierce Protease and Phosphatase Inhibitor Mini Tablets (Life Technologies)). Where detection of KRAS was necessary, cells were lysed in SDS buffer (1 % SDS, 10 mM EDTA, 50 mM Tris, pH 8). Bicinchoninic acid (Sigma) was used to determine protein concentration. Equal amounts of protein were separated by gel electrophoresis, using NuPAGE polyacrylamide gels (Life Technologies). Proteins were transferred to a nitrocellulose membrane using the iBlot 2 system (Life Technologies) and then blocked with LI-COR blocking buffer (LI-COR Biosciences). Membranes were incubated with the primary antibodies overnight at 4 °C, followed by IRdye-conjugated secondary antibodies (LI-COR Biosciences) and detected using an Odyssey Fc imaging system (LI-COR Biosciences). Quantification of Western blots was

performed using Image Studio Lite (LI-COR Biosciences). Details of the antibodies used can be found in **Table S1**.

Lentiviral production

HEK293T cells were seeded at a density of 2.4 x10^6 cells/plate in 10 cm plates. The next day cells were transfected with shRNA/sgRNA plasmid (3 µg) and the packaging plasmids psPAX2 (2.1 µg) and pmD2.G (0.9 µg) using 30 µl lipofectamine per transfection. Cells were incubated for 72 h at 37 °C, after which the supernatant was collected and stored in 0.5 ml aliquots at -80 °C for future experiments. Each batch of lentivirus was titrated on cells to determine concentration needed for 100 % infection efficiency.

shRNA

MISSION shRNA plasmids (pLKO.1) were obtained from Sigma-Aldrich. The pLKO.1-LacZ and -Luciferase targeting shRNA plasmids were from the Genetic Perturbation Platform (The Broad Institute). TRC numbers and target sequences for shRNA plasmids are shown in **Table S2**. Cells were transduced with lentivirus as previously described (19). Cell proliferation was quantified using CellTiter-Blue reagent (Promega) and normalised to cells transduced with control lentivirus. Gene dependency scores were calculated based on the dependency index described by Singh *et al.* (21).

Drug combination screen

Cells were plated in 384 well plates and the Echo 550 Liquid Handler (Labcyte) was used to dispense 20 nl of each compound from a library of 485 Food and Drug Administration approved drugs and tool compounds (selected by the Cancer Research UK Cancer Therapeutics Unit and purchased from Selleckchem) onto the plates to give the final concentration of 800 nM on the cells. Plates were then treated with either 100 nl of DMSO, BYL719 or GDC0941, to give a final concentration of 10 µM BYL719 or 1 µM GDC0941. After a 96 h incubation period, cell proliferation was quantified using CellTiter-Blue reagent (Promega). Synergy was calculated using the Bliss independence model, as previously described. The Bliss score for each combination is the mean of three replicates.

CRISPR

LentiCRISPRv2 (was a gift from Feng Zhang, Addgene plasmid #52961) (22) were digested with *Esp3*I at 37 °C overnight (New England Biolabs, NEB). Oligos were designed to include each sgRNA target sequence (**Table S3**) according to the “Zhang Lab General Cloning Protocol”, available at https://www.addgene.org/crispr/zhang/. Each pair of oligos

was phosphorylated and annealed with T4 PNK enzyme (NEB). Each oligo duplex was then ligated into the appropriate vector using the quick ligase enzyme (NEB) at 16 °C overnight. Lentiviral plasmids were transformed into Stbl3 bacteria (Invitrogen), according to the manufacturer's instructions and then plated on ampicillin (50 mg/ml)-selective agar plates. Single colonies were then amplified, extracted and used to produce lentivirus as described above. Before generation of lentivirus, each amplified plasmid was sequenced to ensure successful sgRNA sequence integration. To generate clonal cell populations expressing each plasmid, cells were first transduced with the virus. Cells were transduced with the lentiCRISPRv2 lentivirus, as this also contains the vector for Cas9 expression. Cells successfully transduced with lentiCRISPRv2 were selected for using 10 µg/ml blasticidin, respectively. After 7 d of selection, cells were seeded in 96 well plates at a density of 0.5 cells/well to select for clonal populations. These were expanded under continued antibiotic selection until sufficient cell numbers were generated. Stocks were frozen down in FBS with 10 % DMSO and stored in liquid nitrogen.

Generation of Cas9 cell lines

Cell lines were engineered to express Cas9 by centrifugation of $4x10^6$ cells with (pXPR101) Cas9 lentivirus (1:1), in the presence of 8 µg/ml polybrene for 1 h at 37 °C. Cells were incubated with fresh media overnight, before cells were trypsinized and pooled for selection. Cells were incubated with 10 µg/ml blasticidin for 7 d to select for successfully infected cells. In parallel, cells were plated in 6 well plates for determination of infection efficiency. To assess Cas9 activity, parental and Cas9 expressing cells were infected with a lentivirus encoding both EGFP and a sgRNA targeting EGFP (pXPR_011-sgEGFP). Successfully transduced cells were selected for using 2 µg/ml puromycin, until all cells of a 'no infection control' were dead. Cells were assayed by flow cytometry to assess EGFP expression. The activity of Cas9 was taken as the proportion of EGFP negative cells in the Cas9 transduced population.

Genome-wide synthetic lethal screen protocol

Cells were seeded in 12 well plates at a density of $3x10^6$ cells/well in 2 ml media. Cells were infected with the Avana4 lentiviral library (Broad Institute, 74,687 sgRNAs targeting 18,407 genes, (23,24)) in four infection replicates. Cells were infected with a predicted representation of 500 cells/sgRNA after selection and with the volume of virus/well that gave ~40 % infection efficiency. Cells were centrifuged at 2000 rpm for 2 h at 30 °C in the presence of lentivirus and 8 µg/ml polybrene, followed by incubation in fresh media overnight. Cells were pooled and seeded into T225 flasks at a density of $1x10^7$ cells/flask for selection with 2 µg/ml puromycin for 7 d and passaged as necessary. In parallel, cells were

seeded in 6 well plates to determine infection efficiency. After 7 d of selection, MIAPACA2 cells were split into three arms and treated with either 0.02 % DMSO, 10 μM BYL719 or 1 μM GDC0941. Throughout the screen cells were passaged as necessary, maintaining a total representation of 500 cells/sgRNA in each replicate. After 8 population doublings, cells from each arm were collected and cell pellets stored at -80 °C. Genomic DNA was extracted using the QIAamp DNA Blood Maxi Kit (Qiagen). PCR amplification and next generation sequencing was conducted as previously described (23). Briefly, sequencing adaptors and sample barcodes were added to sgRNA sequences from gDNA and pDNA samples by PCR. Samples were purified with Agencourt AMPure XP SPRI beads (Beckman Coulter A63880) and then sequenced on a HiSeq2000 (Illumina). Reads were counted by searching for the CACCG sequence of each sgRNA insert and then mapping the 20 nucleotide sgRNA sequence to a reference file of all sgRNAs in the library and assigned to the treatment condition based on the appended barcode.

Focussed minipool screen protocol

The custom minipool lentiviral library (3,067 sgRNAs targeting 296 top hit genes (one gene was accidentally omitted), 496 non-targeting control sgRNAs and 201 sgRNAs targeting essential genes) was prepared as previously described (23,24). Plasmid DNA (pDNA) was sequenced by next-generation sequencing (NGS) to quantify the abundance of each sgRNA in the pool. The pDNA pool was then transfected into HEK 293T cells to produce lentivirus according to the “Large Scale Lentiviral Production” protocol available at https://portals.broadinstitute.org/gpp/public/resources/protocols. Each cell line was infected with the custom minipool lentiviral library in four infection replicates. Cells were infected with a predicted representation of 2000 cells/sgRNA, after selection, and with the volume of virus/well that gave ~40 % infection efficiency, as determined previously. The transduction and selection protocol used was the same as in the genome-wide screen and is described above. After 7 d of selection, cells were split into three arms and treated with either 0.02 % DMSO, BYL719 or GDC0941. Throughout the screen cells were passaged to maintain a representation of 2000 cells/sgRNA. After 8 population doublings, cells from each arm were collected and genomic DNA was extracted and sequenced, as in the whole-genome screen.

CRISPR screen analysis

The abundance of each sgRNA in each replicate was quantified by calculating the Log_2(sequencing reads/million) (RPM), according to the formula below.

$$\mathbf{RPM = Log_2\left(\left(\left(reads\ per\ sgRNA / total\ reads\ per\ condition\right) \times 10^6\right) + 1\right)}$$

The $\log_2$ fold change (LFC) from the early time point was calculated by normalising RPM for each sgRNA in each replicate to that in an early time point control taken 3 d after selection with puromycin. The LFC between the DMSO and drug treated arms was calculated as the difference in average LFC across 3 replicates. This was used to rank individual sgRNAs according to their selective depletion or enrichment in the drug treated arms. Top scoring genes were ranked according to the number of independent high scoring sgRNAs targeting the same gene, according to the STARS gene-ranking algorithm (23). In order to assess depletion of essential genes from the population, as a positive control for successful gene editing, the RPM for each sgRNA was normalised to the plasmid DNA to calculate the LFC from baseline. The list of 885 core essential genes was kindly provided by Dr Marco Licciardello (The Institute of Cancer Research) and is compiled from the genes that were consistently and significantly depleted in all cell lines tested from three previous publications (25-27). To assess the statistical significance of the overlap between genes that modulated the response to BYL719 or GDC0941, the representation factor was calculated as below.

The associated probability was calculated by exact hypergeometric probability as detailed at

$$\textbf{Representation factor} = \frac{\textbf{\# genes in common}}{\textbf{expected \# of genes}}$$

$$\textbf{Expected \# of genes} = \frac{\textbf{(\# genes in group 1 * \# genes in group 2)}}{\textbf{Total number of genes tested}}$$

http://nemates.org/MA/progs/representation.stats.html.

Gene set enrichment analysis of genome-wide screen

A list of all hit genes was compiled from those that were that were enriched or depleted from the BYL719 or GDC0941 treated arms of the genome-wide CRISPR screen (FDR <0.3). This list was used to interrogate the Reactome (28) and KEGG (29,30) gene sets within the Molecular signatures database (31,32), available at http://software.broadinstitute.org/gsea/msigdb.

Results

Loss of function CRISPR screen in PDAC cells identifies RTK and mTOR signalling networks as key determinants of response to PI3K inhibition

To discover loss of function events that modulate sensitivity to PI3K inhibition in PDAC we conducted a genome-wide CRISPR screen anchored to the PI3Kα-selective inhibitor BYL719 (alpelisib)(33) or the pan-class I PI3K inhibitor GDC0941 (pictilisib)(34). *In vitro,* pancreatic cell lines were resistant to BYL719 and GDC0941, compared to the PI3Kα-

dependent breast cancer cell line, T47D (**Figure 1A, S1A**)(35). Resistance was observed despite inhibition of PI3K-AKT signalling, highlighting a disconnect between pathway inhibition and inhibition of cell proliferation in the pancreatic cells (**Figure 1B, S1E**). We selected MIAPACA2 cells for the genome-wide screen, as they were resistant to both BYL719 and GDC0941 and dependent on KRAS for proliferation (**Figure S1A-C**). We engineered this cell line to stably express Cas9 (MIAPACA2_Cas9) and confirmed that Cas9 expression did not alter the response to PI3K inhibition by BYL719 or the pan-PI3K inhibitor GDC0941 (**Figures S1D-E**).

MIAPACA2_Cas9 cells were transduced with Avana4 lentiviral library (23,24). Cells were split into DMSO-, BYL719- or GDC0941-treated arms and passaged for 8 population doublings (**Figure 1C**). Cell proliferation rate was slowed by incubation with 10 μM BYL719 or 1 μM GDC0941 (**Figure 1D**), concentrations at which PI3K signalling was near-completely inhibited. Our choice of inhibitor concentration was driven by a balance of attaining near-complete pathway inhibition at a concentration that permits sufficient cell proliferation for the screen to be performed within approximately 3-4 weeks. Although the concentration of BYL719 used was quite high, we hypothesised that by using two chemically distinct inhibitors, off-target effects could be accounted for by focusing on hits observed with both inhibitors. Cells were harvested, genomic DNA (gDNA) extracted and sgRNAs amplified and barcoded by PCR. Next generation sequencing (NGS) was employed to quantify the abundance of each sgRNA in each experimental arm. This analysis demonstrated that sgRNAs targeting essential genes or KRAS, a known dependency of this cell line, were depleted from the population, whereas non-targeting sgRNAs were not (**Figure S2A**). The STARS algorithm (23,24) was used to rank genes with multiple scoring sgRNAs that were selectively depleted (enhancers of the antiproliferative effect) or enriched (suppressors of the antiproliferative effect) in each arm of the screen compared to DMSO (**Figure 1E-F, Figure S2B-C and Tables S4-7)**.

Overall, there was a large degree of overlap among the hit genes (false discovery rate (FDR) of <0.3) for which sgRNAs were depleted or enriched with BYL719 or GDC0941 treatment (**Figure 1G, Table S8**). Out of 82 and 34 genes for which sgRNAs enhanced the anti-proliferative effect in the BYL719- and GDC0941-treated arms, respectively, 11 of the hits were common to both treatment arms (representation factor 75, $p < 1.192 \times 10^{-18}$). There was a greater degree of overlap between the genes for which sgRNAs were enriched with drug treatment, with 63 genes common to both drugs, out of a total of 135 and 120 genes that were enriched with BYL719 and GDC0941, respectively (representation factor of 74, $p < 6.147 \times 10^{-109}$). Strikingly, sgRNAs targeting multiple negative regulators of PI3K/mTOR signalling were enriched in the drug-treated populations, implying that loss of these genes

promotes resistance to PI3K inhibition. Indeed, the top-ranking sgRNAs that were enriched in both drug-treated arms targeted *TSC1* and *TSC2*, which inhibit the activity of RHEB and downstream mTORC1 signalling (36). Other sgRNAs enriched under drug treatment targeted *PTEN, DDIT4* (36)*, AKT1S1* (37)*,* and *RALGAPB* (38). Guide RNAs targeting genes encoding proteins of the mTORC1 network, mTOR kinase, RAPTOR and RRAGC were significantly depleted from the BYL719-treated arm, suggesting that loss of mTORC1 sensitises cells to BYL719 treatment (39,40). This implicates the mTORC1 complex as a key mediator of resistance to PI3K inhibition. Given that loss of PTEN, TSC1 or TSC2 confers resistance to PI3K inhibition and loss of MTOR sensitizes to PI3K inhibition, this provides important validation of the screening conditions, as these events are known to modulate sensitivity to PI3K inhibitors (41,42).

We used the Molecular Signatures Database (MSigDB) (31,32) to investigate the 297 genes that modulated response to either BYL719 or GDC0941 and found enrichment for multiple pathways involved in PI3K signalling, including mTOR, AKT (PKB) and insulin signalling (**Figure 1H**). Multiple RTK signalling pathways, including the ERBB-family (in particular EGFR and ERBB2) as well as FGFR and PDGF, were enriched among the hit genes that were significantly enriched or depleted from the genome-wide CRISPR screen (FDR<0.3).

'Signalling by EGFR in cancer' was the most highly enriched pathway and is of particular interest in pancreatic cancer as the EGFR inhibitor erlotinib has shown some modest activity in pancreatic cancer patients (43). Moreover, guides targeting genes associated with the internalisation and degradation of activated ERBB-family receptors were enriched in the drug-treated populations. Suppressor hit genes included *AP2S1*, *AP2B1* and *AP2M1,* which encode subunits of the adaptor protein 2 (AP-2) complex and are involved in clathrin-dependent endocytosis of activated EGFR (44). We hypothesise that loss of the AP-2 complex would result in sustained EGFR signalling. *PRKACA* encodes a catalytic subunit of protein kinase A (PKA) which phosphorylates and inhibits EGFR (45) and facilitates its internalisation and ubiquitination (46). Overall, loss of these genes may result in activation of EGFR, thereby promoting resistance to PI3K inhibition.

Minipool validation screen further implicates RTK signalling as a modulator of sensitivity to PI3K inhibition in multiple cell lines.

Penetrant synthetic lethal interactions, which demonstrate similar effects across diverse cellular models, may have greater therapeutic benefit as they could overcome the molecular heterogeneity that exists within tumours (47). Therefore, to prioritise penetrant synthetic lethal effects, we generated a minipool targeting 296 hit genes from the genome

wide screen, including those hits identified with either BYL719 or GDC0941, for a secondary validation screen. We tested this library in MIAPACA2 cells and in 3 additional *KRAS*-mutant pancreatic cancer cell lines. All cell lines chosen for the validation screen were of the QM subtype of PDAC as this represents the subtype with the poorest prognosis and therefore the most urgent clinical unmet need (48). We confirmed that Cas9 expression did not alter response to PI3K inhibition (**Figure S3A)**. We selected concentrations of BYL719 and GDC0941 that inhibited PI3K signalling but still permitted cell proliferation (**Figure S3B**). Cells were then transduced with the minipool library. After puromycin selection, cells were treated with DMSO, BYL719 or GDC0941 and passaged for approximately 8 population doublings (**Figure S4A**). sgRNA abundance was determined as in the whole-genome screen. For each cell line, the abundance of non-targeting sgRNAs was not changed compared to the plasmid DNA, but sgRNAs targeting essential genes were depleted, indicating that transduction led to successful gene editing (**Figure S4B**).

STARS analysis was used to prioritise genes with multiple top-scoring sgRNAs that were either enriched or depleted from the drug treated arms (**Tables S9-24**). To discover penetrant hits, genes were ranked according to their average STARS score across all 4 cell lines (**Figure 2A**). Reassuringly, there was considerable overlap between the hit genes that could modulate sensitivity to BYL719 and GDC0941. *MEMO1, UBE2H, MIOS* and *YPEL5* were the top four hit genes that, when lost, sensitised to both BYL719 and GDC0941 across all four cell lines. Targeting of *PTEN, TSC1, TSC2, FRYL, PDCD10* and *NF2* were the top six hit genes that drove resistance to both PI3K inhibitors. Notably, sgRNAs targeting *KEAP1* were enriched in the presence of PI3K inhibition suggesting resistance could also be driven by NFE2L2/NRF2-mediated activation of an antioxidant stress response pathway (49). As STARS only uses the top 10% of sgRNAs to rank genes we also analysed the minipool screen based on the average LFC of all sgRNAs for each cell line and then ranked each gene in the minipool based on the average LFC across all cell lines. Reassuringly, both analysis approaches showed agreement (**Figure S4C**). We also confirmed that sgRNAs targeting the top-ranking genes identified in the primary screen also showed significant enrichment or depletion in the MIAPACA2 cell line in the secondary screen (**Figure S4D**). This suggested good concordance between the primary and secondary screens in MIAPACA2 cells.

We focussed on two hits – MEMO1 and UBE2H, as they were both related to ERBB family signalling. Knockout of MEMO1 or UBE2H by CRISPR/Cas9 was confirmed (**Figure 2B**) and enhanced the antiproliferative effect of BYL719 in PANC03.27 and MIAPACA2 (**Figure 2C**). Both MEMO1 and UBE2H regulate signal transduction by the ERBB family and IGF1R (50,51); therefore, we hypothesised that stimulation of RTKs with specific ligands

could promote resistance to PI3K inhibition. Firstly, by culturing cells in low serum (0.1% FBS) AKT, PRAS40 and S6 phosphorylation were all decreased (**Figure S5A**), suggesting removal of growth factors could dampen signalling, even in the setting of oncogenic KRAS. Furthermore, co-treatment with BYL719 caused a near-complete suppression of AKT, PRAS40 and S6 phosphorylation. Low serum reduced cell proliferation by approximately 50% relative to 10% serum as did treatment with BYL719 (**Figure S5B**). Low serum and BYL719 treatment modestly suppressed cell proliferation further but to a lesser degree compared to drug treatment in 10% serum. This may reflect either the reduced proliferation rate of the cells in low serum and/or a decrease in PI3K signalling under low serum conditions. Interestingly the addition of epidermal growth factor (EGF), heregulin (HRG) and insulin-like growth factor 1 (IGF1) significantly increased the GI_{50} concentration for BYL719 (**Figure 2D**). HRG conferred the greatest degree of resistance to BYL719, associated with sustained AKT and S6 phosphorylation in the presence of BYL719 (**Figure 2E**). Notably, despite EGF strongly activating the EGFR receptor and causing the expected downregulation of EGFR expression (52), it was not as effective as HRG in driving resistance to BYL719. Taken together, these data suggest that the ERBB-family can drive resistance to PI3K inhibition in PDAC cells.

Combination drug screen nominates clinically relevant inhibitors of ERBB and mTOR signalling as sensitizers to PI3K inhibition

To identify clinically relevant inhibitors of RTK signalling that synergized with PI3K inhibition, we used an established library of 485 FDA approved drugs and tool compounds, alone and in combination with 10 μM BYL719 or 1 μM GDC0941. The library was screened in MIAPACA2 cells at a concentration of 800 nM, a concentration empirically chosen for a balance between being sufficient to modulate the target in cells but not so high as to induce off target effects. Nevertheless, some synergistic interactions may not be detected for those compounds which were used at a too high or too low concentration. The Bliss independence model (20) was used to calculate synergy for each drug combination (**Tables S25-26**). To identify hits common to both PI3K inhibitors, the Bliss score for BYL719 was plotted against that for GDC0941 (**Figure 3A**). The compounds were also ranked based on their average Bliss score for both PI3K inhibitors (**Figure 3B**). Notably, the ERBB family inhibitor pelitinib demonstrated greatest synergy with both PI3K inhibitors. Another ERBB family inhibitor, dacomitinib, also demonstrated synergy with both compounds. Multiple inhibitors of mTOR also ranked highly, including KU-0063794, rapamycin, ridaforolimus, everolimus and WYE-354. KU-0063794 inhibits mTORC1 and mTORC2 kinase activity and, given that it drove greater synergy than mTORC1 allosteric inhibitors such as rapamycin, suggests that dual mTORC1/2 inhibitors may elicit greater synergy with PI3K inhibitors. The ERBB-family

inhibitor, pelitinib (53) and the mTORC1/2 kinase inhibitor, AZD2014 (54) were selected to validate the synergistic interaction between inhibition of PI3K and ERBB or mTOR signalling. The combination of BYL719 and pelitinib or AZD2014 synergistically inhibited proliferation of pancreatic cells in both short- (**Figure 3C**) and long-term (**Figure 3D**) assays. This highlighted the capacity of the ERRB-family and the mTOR pathway to drive resistance to PI3K inhibition.

Using a spheroid co-culture of MIAPACA2 cells with activated pancreatic stellate cells (PSCs) — thought to better-model tumor-stromal interactions and the 3D tumor environment *in vivo* compared to 2D culture on plastic (55,56), the combination of BYL719 and pelitinib or AZD2014 robustly inhibited spheroid growth (**Figures 3E&F**). Propidium iodide staining of spheroids after 4 days of treatment demonstrated a significant increase in dead or dying cells with the combination of BYL719 with either pelitinib or AZD2014 versus single agents (**Figure 4G**). Overall, we have clearly demonstrated that combined inhibition of PI3Kα and either ERBB or mTOR is synergistic in multiple models of PDAC.

Resistance to PI3K inhibition is associated with sustained mTORC1 activity and can be overcome with mTOR and ERBB-family inhibitors

The CRISPR and drug combination screens suggested that under PI3Kα inhibition, pancreatic cancer cells depend on mTOR signalling for proliferation. Therefore, we hypothesised that inadequate suppression of mTORC1 signalling underlies the resistance of pancreatic cells to BYL719. Indeed, phosphorylation of S6 (Ser240/244, catalysed by $p70^{S6K}$) was not suppressed by BYL719 treatment in resistant PDAC cells, but was seen in the sensitive breast cancer cell line, T47D, whereas phospho-AKT was suppressed in both the sensitive and insensitive lines (**Figure 4A**). Moreover, while CRISPR-knockout of p110α decreased phosphorylation of AKT (Ser473) and PRAS40 (Thr246), phosphorylation of S6 (Ser240/244) was maintained (**Figure 4A**). Across a panel of 12 pancreatic cell lines, the inhibition of phospho-S6 (Ser240/244) achieved with 10 μM BYL719 closely correlated with the effect on cell proliferation (**Figure 4B**). This suggests that mTOR signalling is uncoupled from PI3K in pancreatic cell lines and that this limits response to PI3Kα inhibition. Hence, we suggest that inhibition of phospho-S6 (Ser240/244) is an important and independent predictor of response to BYL719 versus other more proximal markers of PI3K signalling.

Our results suggest that inhibition of PI3K alone does not inhibit proliferation and that combination with mTORC1 inhibition is required. However, clinical trials of allosteric mTOR inhibitors in pancreatic cancer have been unsuccessful likely due to loss of negative feedback on IRS1 (7,16) and, as shown herein, pancreatic cancer cells are resistant to single agent inhibition of mTORC1 *in vitro* (**Figure S6A**), despite suppression of S6

phosphorylation (**Figure S6B**). We propose that inhibition of both PI3K and mTORC1 signalling is essential to inhibit cell proliferation. In line with this, the mTORC1/2 kinase inhibitors dactolisib (BEZ235) and AZD8055 (a closely-related analog of AZD2014) displayed potent antiproliferative activity in pancreatic cancer cell lines (**Figure S6C&D**) and this was associated with inhibition of phospho-S6 (Ser240/244) and at approximately 10-fold higher concentrations, inhibition of phospho-AKT (Ser473), as expected by dual inhibition of mTORC1 and mTORC2 (**Figure S6E&F**).

We studied the effect of the combinations of BYL719 with pelitinib or AZD2014 on PI3K-mTOR signalling. BYL719 alone resulted in near-complete suppression of phospho-AKT (Ser473) but decreases in phospho-S6 (Ser240/244) were not sustained. (**Figure 4C, Figure S7A&B**). Similarly, AZD2014 or pelitinib could not sustain inhibition of both PI3K-AKT and mTORC1 signalling for 72 h. Only the combination of these agents with BYL719 was sufficient to durably inhibit signalling at both nodes (**Figure 4C, Figure S7A&B**). Given that inhibition of ERBB signalling could also decrease MAPK pathway activity we also assessed the effect of pelitinib alone and in combination with BYL719 on ERK1/2 phosphorylation. However, no robust inhibition was observed, suggesting that decreased MAPK pathway activity was not contributing to the antiproliferative activity of this combination (**Figure S7B**).

Genetic alteration of the ERBB-PI3K signalling axis correlates with poor survival of PDAC patients

To seek clinical relevance for our findings, we investigated how expression of selected genes, implicated by both our CRISPR and drug screens, related to clinical outcomes in PDAC by interrogating publicly available TCGA ‘provisional data’ in cBioPortal (57,58). 91% of patients in this dataset have *KRAS*-mutant tumours. Genetic alterations of the ERBB-family & PI3K signalling axis were present in 40% of 149 cases (**Figure 5A**) and associated with poor survival among PDAC patients, with a significant decrease in median survival from 23 months to 16 months (**Figure 5B**). Therefore, genetic alterations in the ERBB-family and PI3K signalling pathways are common in PDAC patients and may contribute to a poor clinical outcome.

Discussion

Overcoming acquired resistance to targeted therapies is arguably the major challenge facing drug discovery for the treatment of cancer. As exemplified by our CRISPR and drug combination screens, mechanisms of resistance to PI3K inhibition in PDAC converge on signalling through mTORC1. Incomplete suppression of mTORC1 underlies intrinsic resistance to PI3K inhibition and correlates with drug response. This was also

predictive of response to PI3Kα inhibition in cell lines and patient tumours in PI3K-dependent breast cancer (41). Taken together, this suggests that mTORC1 has utility as a biomarker of PI3K inhibition and loss of mTOR signalling, combined with PI3K inhibition, is necessary to inhibit tumour growth. Interestingly, a drug-modifier CRISPR screen with the KRAS inhibitor MRTX849 also identified MTOR depletion as an enhancer of drug activity and validated the combination of MRTX849 with everolimus and AZD2014. Consistent with our data, near-complete suppression of phospho-S6 was associated with an anti-proliferative effect (6).

Our data suggest that alternative pathways may compensate for PI3K inhibition to reactivate mTORC1. PI3K signalling is regulated by growth factors, as removal of FBS is sufficient to inhibit signalling through AKT and PRAS40 in PDAC cells. EGF confers resistance to BYL719 in head and neck cancer (62) and IGF1 and neuregulin 1 (also known as heregulin, HRG) drive resistance to PI3K inhibition in *PIK3CA*-mutant breast cancer (41). IGF1 is of interest in pancreatic cancer as it is found at high levels in tumour stroma (63). The greatest protective effect was associated with reactivation of PI3K signalling by HRG and suggests that ligand-mediated ERBB family activation participates in driving resistance to PI3K inhibition in PDAC, even in the context of oncogenic *KRAS*.

Numerous regulators of RTK signalling were implicated in resistance to PI3K inhibition in both CRISPR screens. Of these, MEMO1 interacts with IGF1R and all four ERBB-family members (50,51) and mediates activation of MAPK and PI3K signalling (51). MEMO1 also interacts with IRS1 and prevents dephosphorylation and deactivation of IRS1 signalling (50). UBE2H is involved in insulin and PI3K signalling in skeletal muscle and cooperates with the E3-ubiquitin ligase, Mitsugumin 53 (MG53 or TRIM72), to ubiquitinate and downregulate IRS1, which is important for negative feedback regulation of IGF1 and insulin signalling and inhibition of skeletal myogenesis (64). Loss of these genes sensitised cells to PI3K inhibition, demonstrating that RTK signalling is a clear determinant of response to PI3K inhibition.

The combination drug screen suggested that targeting of mTOR or the ERBB-family could circumvent resistance to PI3K inhibition. The ERBB-family consists of four receptor tyrosine kinases, which are activated by ligand binding and regulate the RAS, MAPK and PI3K pathways. (65). However, KRAS is activated downstream of EGFR signalling, implying that EGFR may have little relevance in tumours driven by constitutively activated RAS signalling. In support of this, activating mutations in KRAS drive resistance to EGFR inhibitors in colorectal cancer (66,67). Conversely, in PDAC clinical trials, addition of the EGFR inhibitor, erlotinib, to gemcitabine resulted in a modest survival benefit, suggesting that tumours may still partially rely on EGFR signalling (43). In line with this, we show that

genetic alterations of ERBB and PI3K pathway members in PDAC patient tumours associates with poor survival and may provide potential patient selection criteria for this drug combination which warrants further investigation as a novel therapeutic strategy in PDAC. The use of gene expression signatures, to classify pancreatic cancers into distinct subtypes that exhibit vulnerabilities to specific drugs also has the potential to inform treatment decisions (48). For example, we focussed on the QM subtype of pancreatic cancer, so this patient population would be a rational choice for preliminary investigations. Furthermore, around 50% of clinical pancreatic samples are EGFR positive and overexpression correlates with poor survival (43). Upregulation of EGFR occurs selectively in PanINs and early stages of PDAC in mice (68,69), which implicates this receptor in tumour development. Moreover, mouse models show that *Kras*-driven tumorigenesis is dependent on Egfr, as genetic inactivation of *Egfr* blocks induction of PanINs and PDAC (68,69). Similarly, studies of *KRAS*-mutant NSCLC show that ERBB-family signalling amplifies the activity of mutant KRAS in *in vivo* models and loss of ERBB-family signalling impairs tumour development (70,71). Furthermore, studies conducted with the KRAS inhibitors AMG510 or MRTX849 have shown synergistic antiproliferative activity with ERBB-family inhibitors (5,6). Studies in pancreatic organoid models have shown synergy between either MEK or AKT inhibitors when combined with ERBB-family inhibitors (but not with EGFR inhibition), underscoring the need to completely suppress ERBB signalling for activity (72). Pelitinib is a potent and irreversible EGFR inhibitor that also has activity against other ERBB family members, most notably HER2 (73,74). Therefore, the synergistic activity is likely not due to inhibition of EGFR alone, but through more durable inhibition of all ERBB-family receptors. These data clearly support a role for the ERBB-family in mutant KRAS signalling and KRAS-driven tumorigenesis and cell proliferation across tumour types.

We have shown that pancreatic cancer cell lines are predominantly resistant to inhibition of PI3K via sustained mTOR signalling, despite effective inhibition of upstream PI3K signalling, indicating that alternative pathways can maintain mTORC1 activation and promote proliferation. Our genetic and pharmacological data show that dual inhibition of PI3K and mTORC1 signalling achieves greater antiproliferative activity than targeting a single node. Notably, dual mTORC1/2 kinase inhibitors such as AZD2014 achieve this at low nanomolar concentrations that are pharmacologically-relevant, whereas higher concentrations of mTORC1 allosteric inhibitors are required to achieve similar effects. This suggests a potential benefit of inhibiting both mTORC1 and mTORC2. Furthermore, this can also be achieved by combined inhibition of PI3Kα and ERBB-family signalling, indicating that the ERBB family is important for sustaining mTORC1 activity in the presence of PI3K inhibition, even in the context of mutant KRAS (**Figure S8**). Given the role of ERBB-family

activity in enhancing signalling through KRAS in NSCLC (70,71), one may speculate that inhibition of mTOR, downstream of ERBB-family inhibition, may result from attenuation of RTK-driven wildtype KRAS signalling (75). However, we did not detect robust inhibition of ERK phosphorylation in response to pelitinib (alone or with BYL719), suggesting this was not MAPK-dependent. This study provides the basis for future translational work in xenograft and genetically-engineered mouse models of pancreatic cancer, to determine the tolerability and efficacy of combined PI3K and mTOR kinase inhibitors or irreversible ERBB-family inhibitors. Reassuringly, the combination of PI3K and pan-ERBB inhibitors has been tested in *KRAS* or *PIK3CA*-driven xenografts and GEMMs confirming this therapeutic strategy is tolerated and efficacious *in vivo* (76-78). Our data suggest potential pharmacodynamic biomarkers to monitor drug response and guide dosing strategies. Positive results may renew interest in these classes of therapeutic agents for this challenging cancer type.

Acknowledgments

This work has been funded by The Institute of Cancer Research, Pancreatic Cancer UK and the Louis Nicholas Residuary Charitable Trust (to S.R. Whittaker). We thank Drs Muge Sarper and Amine Sadok at The Institute of Cancer Research for advice on the spheroid, co-culture assays and Drs Mark Stubbs and Rosemary Burke, also at The Institute of Cancer Research, for access to the compound library and assistance with ECHO dispensing.

References

1. Cancer Research UK Cancer Statistics for the UK. http://www.cancerresearchuk.org/health-professional/cancer-statistics/. Accessed June 2018.
2. Cunningham D, Atkin W, Lenz HJ, Lynch HT, Minsky B, Nordlinger B*, et al.* Colorectal cancer. Lancet (London, England) **2010**;375(9719):1030-47 doi 10.1016/s0140-6736(10)60353-4.
3. Witkiewicz AK, McMillan EA, Balaji U, Baek G, Lin WC, Mansour J*, et al.* Whole-exome sequencing of pancreatic cancer defines genetic diversity and therapeutic targets. Nat Commun **2015**;6:6744 doi 10.1038/ncomms7744.
4. Collins MA, Bednar F, Zhang YQ, Brisset JC, Galban S, Galban CJ*, et al.* Oncogenic Kras is required for both the initiation and maintenance of pancreatic cancer in mice. J Clin Invest **2012**;122(2):639-53 doi 10.1172/JCI59227.
5. Canon J, Rex K, Saiki AY, Mohr C, Cooke K, Bagal D*, et al.* The clinical KRAS(G12C) inhibitor AMG 510 drives anti-tumour immunity. Nature **2019**;575(7781):217-23 doi 10.1038/s41586-019-1694-1.
6. Hallin J, Engstrom LD, Hargis L, Calinisan A, Aranda R, Briere DM*, et al.* The KRAS(G12C) Inhibitor MRTX849 Provides Insight toward Therapeutic Susceptibility of KRAS-Mutant Cancers in Mouse Models and Patients. Cancer Discov **2020**;10(1):54-71 doi 10.1158/2159-8290.CD-19-1167.
7. Javle MM, Shroff RT, Xiong H, Varadhachary GA, Fogelman D, Reddy SA*, et al.* Inhibition of the mammalian target of rapamycin (mTOR) in advanced pancreatic cancer: results of two phase II studies. BMC Cancer **2010**;10:368 doi 10.1186/1471-2407-10-368.
8. Edling CE, Selvaggi F, Buus R, Maffucci T, Di Sebastiano P, Friess H*, et al.* Key role of phosphoinositide 3-kinase class IB in pancreatic cancer. Clin Cancer Res **2010**;16(20):4928-37 doi 10.1158/1078-0432.CCR-10-1210.
9. Asano T, Yao Y, Zhu J, Li D, Abbruzzese JL, Reddy SA. The PI 3-kinase/Akt signaling pathway is activated due to aberrant Pten expression and targets transcription factors NF-kappaB and c-Myc in pancreatic cancer cells. Oncogene **2004**;23(53):8571-80 doi 10.1038/sj.onc.1207902.
10. Yuan TL, Cantley LC. PI3K pathway alterations in cancer: variations on a theme. Oncogene **2008**;27(41):5497-510 doi 10.1038/onc.2008.245.
11. Kennedy AL, Morton JP, Manoharan I, Nelson DM, Jamieson NB, Pawlikowski JS*, et al.* Activation of the PIK3CA/AKT pathway suppresses senescence induced by an activated RAS oncogene to promote tumorigenesis. Mol Cell **2011**;42(1):36-49 doi 10.1016/j.molcel.2011.02.020.
12. Morran DC, Wu J, Jamieson NB, Mrowinska A, Kalna G, Karim SA*, et al.* Targeting mTOR dependency in pancreatic cancer. Gut **2014**;63(9):1481-9 doi 10.1136/gutjnl-2013-306202.
13. Gupta S, Ramjaun AR, Haiko P, Wang Y, Warne PH, Nicke B*, et al.* Binding of ras to phosphoinositide 3-kinase p110alpha is required for ras-driven tumorigenesis in mice. Cell **2007**;129(5):957-68 doi 10.1016/j.cell.2007.03.051.
14. Eser S, Reiff N, Messer M, Seidler B, Gottschalk K, Dobler M*, et al.* Selective requirement of PI3K/PDK1 signaling for Kras oncogene-driven pancreatic cell plasticity and cancer. Cancer Cell **2013**;23(3):406-20 doi 10.1016/j.ccr.2013.01.023.
15. Baer R, Cintas C, Dufresne M, Cassant-Sourdy S, Schonhuber N, Planque L*, et al.* Pancreatic cell plasticity and cancer initiation induced by oncogenic Kras is completely dependent on wild-type PI 3-kinase p110alpha. Genes Dev **2014**;28(23):2621-35 doi 10.1101/gad.249409.114.

16. Wolpin BM, Hezel AF, Abrams T, Blaszkowsky LS, Meyerhardt JA, Chan JA*, et al.* Oral mTOR inhibitor everolimus in patients with gemcitabine-refractory metastatic pancreatic cancer. J Clin Oncol **2009**;27(2):193-8 doi 10.1200/JCO.2008.18.9514.
17. She QB, Halilovic E, Ye Q, Zhen W, Shirasawa S, Sasazuki T*, et al.* 4E-BP1 is a key effector of the oncogenic activation of the AKT and ERK signaling pathways that integrates their function in tumors. Cancer Cell **2010**;18(1):39-51 doi 10.1016/j.ccr.2010.05.023.
18. She QB, Solit DB, Ye Q, O'Reilly KE, Lobo J, Rosen N. The BAD protein integrates survival signaling by EGFR/MAPK and PI3K/Akt kinase pathways in PTEN-deficient tumor cells. Cancer Cell **2005**;8(4):287-97 doi 10.1016/j.ccr.2005.09.006.
19. Whittaker SR, Theurillat JP, Van Allen E, Wagle N, Hsiao J, Cowley GS*, et al.* A genome-scale RNA interference screen implicates NF1 loss in resistance to RAF inhibition. Cancer Discov **2013**;3(3):350-62 doi 10.1158/2159-8290.CD-12-0470.
20. Bliss CI. The Toxicity of poisons applied jointly. Annals of Applied Biology **1939**;26(3):585-615 doi 10.1111/j.1744-7348.1939.tb06990.x.
21. Singh A, Greninger P, Rhodes D, Koopman L, Violette S, Bardeesy N*, et al.* A gene expression signature associated with "K-Ras addiction" reveals regulators of EMT and tumor cell survival. Cancer Cell **2009**;15(6):489-500 doi 10.1016/j.ccr.2009.03.022.
22. Sanjana NE, Shalem O, Zhang F. Improved vectors and genome-wide libraries for CRISPR screening. Nat Methods **2014**;11(8):783-4 doi 10.1038/nmeth.3047.
23. Doench JG, Fusi N, Sullender M, Hegde M, Vaimberg EW, Donovan KF*, et al.* Optimized sgRNA design to maximize activity and minimize off-target effects of CRISPR-Cas9. Nat Biotechnol **2016**;34(2):184-91 doi 10.1038/nbt.3437.
24. Piccioni F, Younger ST, Root DE. Pooled Lentiviral-Delivery Genetic Screens. Curr Protoc Mol Biol **2018**;121:32 1 1- 1 21 doi 10.1002/cpmb.52.
25. Blomen VA, Majek P, Jae LT, Bigenzahn JW, Nieuwenhuis J, Staring J*, et al.* Gene essentiality and synthetic lethality in haploid human cells. Science **2015**;350(6264):1092-6 doi 10.1126/science.aac7557.
26. Hart T, Chandrashekhar M, Aregger M, Steinhart Z, Brown KR, MacLeod G*, et al.* High-Resolution CRISPR Screens Reveal Fitness Genes and Genotype-Specific Cancer Liabilities. Cell **2015**;163(6):1515-26 doi 10.1016/j.cell.2015.11.015.
27. Wang T, Birsoy K, Hughes NW, Krupczak KM, Post Y, Wei JJ*, et al.* Identification and characterization of essential genes in the human genome. Science **2015**;350(6264):1096-101 doi 10.1126/science.aac7041.
28. Fabregat A, Jupe S, Matthews L, Sidiropoulos K, Gillespie M, Garapati P*, et al.* The Reactome Pathway Knowledgebase. Nucleic Acids Res **2018**;46(D1):D649-D55 doi 10.1093/nar/gkx1132.
29. Kanehisa M, Furumichi M, Tanabe M, Sato Y, Morishima K. KEGG: new perspectives on genomes, pathways, diseases and drugs. Nucleic Acids Res **2017**;45(D1):D353-D61 doi 10.1093/nar/gkw1092.
30. Kanehisa M, Goto S. KEGG: kyoto encyclopedia of genes and genomes. Nucleic Acids Res **2000**;28(1):27-30.
31. Liberzon A, Subramanian A, Pinchback R, Thorvaldsdottir H, Tamayo P, Mesirov JP. Molecular signatures database (MSigDB) 3.0. Bioinformatics **2011**;27(12):1739-40 doi 10.1093/bioinformatics/btr260.
32. Subramanian A, Tamayo P, Mootha VK, Mukherjee S, Ebert BL, Gillette MA*, et al.* Gene set enrichment analysis: a knowledge-based approach for interpreting genome-wide expression profiles. Proc Natl Acad Sci U S A **2005**;102(43):15545-50 doi 10.1073/pnas.0506580102.
33. Furet P, Guagnano V, Fairhurst RA, Imbach-Weese P, Bruce I, Knapp M*, et al.* Discovery of NVP-BYL719 a potent and selective phosphatidylinositol-3 kinase alpha inhibitor selected for clinical evaluation. Bioorg Med Chem Lett **2013**;23(13):3741-8 doi 10.1016/j.bmcl.2013.05.007.

34. Folkes AJ, Ahmadi K, Alderton WK, Alix S, Baker SJ, Box G*, et al.* The identification of 2-(1H-indazol-4-yl)-6-(4-methanesulfonyl-piperazin-1-ylmethyl)-4-morpholin-4-yl-thieno[3,2-d]pyrimidine (GDC-0941) as a potent, selective, orally bioavailable inhibitor of class I PI3 kinase for the treatment of cancer. J Med Chem **2008**;51(18):5522-32 doi 10.1021/jm800295d.
35. Fritsch C, Huang A, Chatenay-Rivauday C, Schnell C, Reddy A, Liu M*, et al.* Characterization of the novel and specific PI3Kalpha inhibitor NVP-BYL719 and development of the patient stratification strategy for clinical trials. Mol Cancer Ther **2014**;13(5):1117-29 doi 10.1158/1535-7163.MCT-13-0865.
36. Huang J, Manning BD. The TSC1-TSC2 complex: a molecular switchboard controlling cell growth. Biochem J **2008**;412(2):179-90 doi 10.1042/BJ20080281.
37. Sancak Y, Thoreen CC, Peterson TR, Lindquist RA, Kang SA, Spooner E*, et al.* PRAS40 is an insulin-regulated inhibitor of the mTORC1 protein kinase. Mol Cell **2007**;25(6):903-15 doi 10.1016/j.molcel.2007.03.003.
38. Martin TD, Chen XW, Kaplan RE, Saltiel AR, Walker CL, Reiner DJ*, et al.* Ral and Rheb GTPase activating proteins integrate mTOR and GTPase signaling in aging, autophagy, and tumor cell invasion. Mol Cell **2014**;53(2):209-20 doi 10.1016/j.molcel.2013.12.004.
39. Sancak Y, Bar-Peled L, Zoncu R, Markhard AL, Nada S, Sabatini DM. Ragulator-Rag complex targets mTORC1 to the lysosomal surface and is necessary for its activation by amino acids. Cell **2010**;141(2):290-303 doi 10.1016/j.cell.2010.02.024.
40. Sancak Y, Peterson TR, Shaul YD, Lindquist RA, Thoreen CC, Bar-Peled L*, et al.* The Rag GTPases bind raptor and mediate amino acid signaling to mTORC1. Science **2008**;320(5882):1496-501 doi 10.1126/science.1157535.
41. Elkabets M, Vora S, Juric D, Morse N, Mino-Kenudson M, Muranen T*, et al.* mTORC1 inhibition is required for sensitivity to PI3K p110alpha inhibitors in PIK3CA-mutant breast cancer. Sci Transl Med **2013**;5(196):196ra99 doi 10.1126/scitranslmed.3005747.
42. Juric D, Castel P, Griffith M, Griffith OL, Won HH, Ellis H*, et al.* Convergent loss of PTEN leads to clinical resistance to a PI(3)Kalpha inhibitor. Nature **2015**;518(7538):240-4 doi 10.1038/nature13948.
43. Moore MJ, Goldstein D, Hamm J, Figer A, Hecht JR, Gallinger S*, et al.* Erlotinib plus gemcitabine compared with gemcitabine alone in patients with advanced pancreatic cancer: a phase III trial of the National Cancer Institute of Canada Clinical Trials Group. J Clin Oncol **2007**;25(15):1960-6 doi 10.1200/JCO.2006.07.9525.
44. Rappoport JZ, Simon SM. Endocytic trafficking of activated EGFR is AP-2 dependent and occurs through preformed clathrin spots. J Cell Sci **2009**;122(Pt 9):1301-5 doi 10.1242/jcs.040030.
45. Barbier AJ, Poppleton HM, Yigzaw Y, Mullenix JB, Wiepz GJ, Bertics PJ*, et al.* Transmodulation of epidermal growth factor receptor function by cyclic AMP-dependent protein kinase. J Biol Chem **1999**;274(20):14067-73.
46. Salazar G, Gonzalez A. Novel mechanism for regulation of epidermal growth factor receptor endocytosis revealed by protein kinase A inhibition. Mol Biol Cell **2002**;13(5):1677-93 doi 10.1091/mbc.01-08-0403.
47. Brough R, Gulati A, Haider S, Kumar R, Campbell J, Knudsen E*, et al.* Identification of highly penetrant Rb-related synthetic lethal interactions in triple negative breast cancer. Oncogene **2018** doi 10.1038/s41388-018-0368-z.
48. Collisson EA, Sadanandam A, Olson P, Gibb WJ, Truitt M, Gu S*, et al.* Subtypes of pancreatic ductal adenocarcinoma and their differing responses to therapy. Nat Med **2011**;17(4):500-3 doi 10.1038/nm.2344.
49. Port J, Muthalagu N, Raja M, Ceteci F, Monteverde T, Kruspig B*, et al.* Colorectal Tumors Require NUAK1 for Protection from Oxidative Stress. Cancer Discov **2018**;8(5):632-47 doi 10.1158/2159-8290.CD-17-0533.

50. Sorokin AV, Chen J. MEMO1, a new IRS1-interacting protein, induces epithelial-mesenchymal transition in mammary epithelial cells. Oncogene **2013**;32(26):3130-8 doi 10.1038/onc.2012.327.
51. Jiang K, Yang Z, Cheng L, Wang S, Ning K, Zhou L*, et al.* Mediator of ERBB2-driven cell motility (MEMO) promotes extranuclear estrogen receptor signaling involving the growth factor receptors IGF1R and ERBB2. J Biol Chem **2013**;288(34):24590-9 doi 10.1074/jbc.M113.467837.
52. Heldin CH, Westermark B, Wasteson A. Desensitisation of cultured glial cells to epidermal growth factor by receptor down-regulation. Nature **1979**;282(5737):419-20 doi 10.1038/282419a0.
53. Erlichman C, Hidalgo M, Boni JP, Martins P, Quinn SE, Zacharchuk C*, et al.* Phase I study of EKB-569, an irreversible inhibitor of the epidermal growth factor receptor, in patients with advanced solid tumors. J Clin Oncol **2006**;24(15):2252-60 doi 10.1200/JCO.2005.01.8960.
54. Pike KG, Malagu K, Hummersone MG, Menear KA, Duggan HM, Gomez S*, et al.* Optimization of potent and selective dual mTORC1 and mTORC2 inhibitors: the discovery of AZD8055 and AZD2014. Bioorg Med Chem Lett **2013**;23(5):1212-6 doi 10.1016/j.bmcl.2013.01.019.
55. Gaviraghi M, Tunici P, Valensin S, Rossi M, Giordano C, Magnoni L*, et al.* Pancreatic cancer spheres are more than just aggregates of stem marker-positive cells. Biosci Rep **2011**;31(1):45-55 doi 10.1042/BSR20100018.
56. Tape CJ, Ling S, Dimitriadi M, McMahon KM, Worboys JD, Leong HS*, et al.* Oncogenic KRAS Regulates Tumor Cell Signaling via Stromal Reciprocation. Cell **2016**;165(4):910-20 doi 10.1016/j.cell.2016.03.029.
57. Cerami E, Gao J, Dogrusoz U, Gross BE, Sumer SO, Aksoy BA*, et al.* The cBio cancer genomics portal: an open platform for exploring multidimensional cancer genomics data. Cancer Discov **2012**;2(5):401-4 doi 10.1158/2159-8290.CD-12-0095.
58. Gao J, Aksoy BA, Dogrusoz U, Dresdner G, Gross B, Sumer SO*, et al.* Integrative analysis of complex cancer genomics and clinical profiles using the cBioPortal. Sci Signal **2013**;6(269):pl1 doi 10.1126/scisignal.2004088.
59. Nazarian R, Shi H, Wang Q, Kong X, Koya RC, Lee H*, et al.* Melanomas acquire resistance to B-RAF(V600E) inhibition by RTK or N-RAS upregulation. Nature **2010**;468(7326):973-7 doi 10.1038/nature09626.
60. Johannessen CM, Boehm JS, Kim SY, Thomas SR, Wardwell L, Johnson LA*, et al.* COT drives resistance to RAF inhibition through MAP kinase pathway reactivation. Nature **2010**;468(7326):968-72 doi 10.1038/nature09627.
61. Arora VK, Schenkein E, Murali R, Subudhi SK, Wongvipat J, Balbas MD*, et al.* Glucocorticoid receptor confers resistance to antiandrogens by bypassing androgen receptor blockade. Cell **2013**;155(6):1309-22 doi 10.1016/j.cell.2013.11.012.
62. Elkabets M, Pazarentzos E, Juric D, Sheng Q, Pelossof RA, Brook S*, et al.* AXL mediates resistance to PI3Kalpha inhibition by activating the EGFR/PKC/mTOR axis in head and neck and esophageal squamous cell carcinomas. Cancer Cell **2015**;27(4):533-46 doi 10.1016/j.ccell.2015.03.010.
63. Bergmann U, Funatomi H, Yokoyama M, Beger HG, Korc M. Insulin-like growth factor I overexpression in human pancreatic cancer: evidence for autocrine and paracrine roles. Cancer Res **1995**;55(10):2007-11.
64. Yi JS, Park JS, Ham YM, Nguyen N, Lee NR, Hong J*, et al.* MG53-induced IRS-1 ubiquitination negatively regulates skeletal myogenesis and insulin signalling. Nat Commun **2013**;4:2354 doi 10.1038/ncomms3354.
65. Yarden Y, Sliwkowski MX. Untangling the ErbB signalling network. Nat Rev Mol Cell Biol **2001**;2(2):127-37 doi 10.1038/35052073.
66. Karapetis CS, Khambata-Ford S, Jonker DJ, O'Callaghan CJ, Tu D, Tebbutt NC*, et al.* K-ras mutations and benefit from cetuximab in advanced colorectal cancer. N Engl J Med **2008**;359(17):1757-65 doi 10.1056/NEJMoa0804385.

67. Van Emburgh BO, Arena S, Siravegna G, Lazzari L, Crisafulli G, Corti G*, et al.* Acquired RAS or EGFR mutations and duration of response to EGFR blockade in colorectal cancer. Nat Commun **2016**;7:13665 doi 10.1038/ncomms13665.
68. Navas C, Hernandez-Porras I, Schuhmacher AJ, Sibilia M, Guerra C, Barbacid M. EGF receptor signaling is essential for k-ras oncogene-driven pancreatic ductal adenocarcinoma. Cancer Cell **2012**;22(3):318-30 doi 10.1016/j.ccr.2012.08.001.
69. Ardito CM, Gruner BM, Takeuchi KK, Lubeseder-Martellato C, Teichmann N, Mazur PK*, et al.* EGF receptor is required for KRAS-induced pancreatic tumorigenesis. Cancer Cell **2012**;22(3):304-17 doi 10.1016/j.ccr.2012.07.024.
70. Kruspig B, Monteverde T, Neidler S, Hock A, Kerr E, Nixon C*, et al.* The ERBB network facilitates KRAS-driven lung tumorigenesis. Sci Transl Med **2018**;10(446) doi 10.1126/scitranslmed.aao2565.
71. Moll HP, Pranz K, Musteanu M, Grabner B, Hruschka N, Mohrherr J*, et al.* Afatinib restrains K-RAS-driven lung tumorigenesis. Sci Transl Med **2018**;10(446) doi 10.1126/scitranslmed.aao2301.
72. Ponz-Sarvise M, Corbo V, Tiriac H, Engle DD, Frese KK, Oni TE*, et al.* Identification of Resistance Pathways Specific to Malignancy Using Organoid Models of Pancreatic Cancer. Clin Cancer Res **2019**;25(22):6742-55 doi 10.1158/1078-0432.CCR-19-1398.
73. Schaefer G, Shao L, Totpal K, Akita RW. Erlotinib directly inhibits HER2 kinase activation and downstream signaling events in intact cells lacking epidermal growth factor receptor expression. Cancer Res **2007**;67(3):1228-38 doi 10.1158/0008-5472.CAN-06-3493.
74. Wissner A, Overbeek E, Reich MF, Floyd MB, Johnson BD, Mamuya N*, et al.* Synthesis and structure-activity relationships of 6,7-disubstituted 4-anilinoquinoline-3-carbonitriles. The design of an orally active, irreversible inhibitor of the tyrosine kinase activity of the epidermal growth factor receptor (EGFR) and the human epidermal growth factor receptor-2 (HER-2). J Med Chem **2003**;46(1):49-63 doi 10.1021/jm020241c.
75. Young A, Lou D, McCormick F. Oncogenic and wild-type Ras play divergent roles in the regulation of mitogen-activated protein kinase signaling. Cancer Discov **2013**;3(1):112-23 doi 10.1158/2159-8290.CD-12-0231.
76. Belmont PJ, Jiang P, McKee TD, Xie T, Isaacson J, Baryla NE*, et al.* Resistance to dual blockade of the kinases PI3K and mTOR in KRAS-mutant colorectal cancer models results in combined sensitivity to inhibition of the receptor tyrosine kinase EGFR. Sci Signal **2014**;7(351):ra107 doi 10.1126/scisignal.2005516.
77. Brady SW, Zhang J, Seok D, Wang H, Yu D. Enhanced PI3K p110alpha signaling confers acquired lapatinib resistance that can be effectively reversed by a p110alpha-selective PI3K inhibitor. Mol Cancer Ther **2014**;13(1):60-70 doi 10.1158/1535-7163.MCT-13-0518.
78. Young CD, Pfefferle AD, Owens P, Kuba MG, Rexer BN, Balko JM*, et al.* Conditional loss of ErbB3 delays mammary gland hyperplasia induced by mutant PIK3CA without affecting mammary tumor latency, gene expression, or signaling. Cancer Res **2013**;73(13):4075-85 doi 10.1158/0008-5472.CAN-12-4579.
79. Bernard V, Kim DU, San Lucas FA, Castillo J, Allenson K, Mulu FC*, et al.* Circulating Nucleic Acids Are Associated With Outcomes of Patients With Pancreatic Cancer. Gastroenterology **2019**;156(1):108-18 e4 doi 10.1053/j.gastro.2018.09.022.
80. San Lucas FA, Allenson K, Bernard V, Castillo J, Kim DU, Ellis K*, et al.* Minimally invasive genomic and transcriptomic profiling of visceral cancers by next-generation sequencing of circulating exosomes. Ann Oncol **2016**;27(4):635-41 doi 10.1093/annonc/mdv604.

Figures

Figure 1. A whole-genome CRISPR screen implicates receptor tyrosine kinase and mTOR signalling networks as modulators of response to PI3K inhibition.

A. Proliferation of 14 human pancreatic cell lines (all *KRAS*-mutant except BxPC3) and one breast cancer cell line (T47D *KRAS* wildtype) was measured after incubation with increasing concentrations of BYL719 for 72 h. Proliferation was quantified using CellTiter-Blue and compound GI_{50} values were calculated using GraphPad Prism. Mean cell proliferation, relative to DMSO control, is plotted ± standard error (n=3).

B. Phosphorylation of AKT and PRAS40 was assessed by Western blotting after incubation with increasing concentrations of BYL719 for 2 h, in the cell lines MIAPACA2, PANC1 and T47D (n=2).

C. Overview of genome-wide CRISPR screening method. Cas9-expressing MIAPACA2 cells were infected with the Avana4 pooled CRISPR library and split into three arms. Cells were passaged for 8 population doublings in the presence of DMSO, BYL719 or GDC0941. The abundance of each sgRNA was assessed by next generation sequencing, under each condition.

D. Following successful transduction of MIAPACA2_Cas9 cells with the Avana4 sgRNA library, cells were cultured in the presence of DMSO, 10 µM BYL719 or 1 µM GDC0941 for at least 8 population doublings. Cells were counted every 3-5 d and population doublings are the mean of four replicates ± SE.

E. The average log-fold change (LFC) in sgRNA abundance was determined for BYL719-treated samples versus the DMSO controls. STARS analysis was used to rank genes that when targeted by CRISPR, enhanced the antiproliferative activity of BYL719.

F. STARS analysis was used as in E to rank genes that when targeted by CRISPR, suppressed the antiproliferative activity of BYL719 and conferred resistance to the drug.

G. Venn diagram analysis of hit genes to identify shared enhancers/suppressors of BYL719 and GDC0941 activity.

H. GSEA highlights key pathways that modulate sensitivity to PI3K inhibition. Significantly enriched pathways from the Reactome and KEGG databases were nominated from a list of the hit genes (FDR < 0.3) that were enriched or depleted in the genome-wide CRISPR screen with either BYL719 or GDC0941.

Figure 2. The ERBB-family can sustain pancreatic cancer cell proliferation and mediate resistance to PI3K inhibition associated with S6 phosphorylation.

A. A secondary screen of top-ranking hits from the primary screen was conducted in MIAPACA2, PANC1, PATU8902 and PANC03.27 cells treated with BYL719 or GDC0941. For each cell line, STARS analysis was used to rank genes that enhanced or suppressed the antiproliferative activity of BYL719 or GDC0941. Genes were then ranked according to the mean STARS score across all four cell lines. Genes with a STARS score of 4 or more in 3 or more cell lines are highlighted in red. Grey boxes indicate the gene was not ranked by STARS.

B. PANC03.27 and MIAPACA2 cells expressing Cas9 were transduced with lentiviral vectors encoding sgRNAs targeting GFP, UBE2H or MEMO1 to generate cell populations with reduced expression of either UBE2H or MEMO1. Cells were lysed 7 d after transfection and cell lysates were analyzed by Western blotting (n=3).

C. Cells as in B were treated with increasing concentrations of BYL719 or GDC0941. After 4 d of drug treatment, cell proliferation was quantified using CellTiter-Blue. Mean cell proliferation, relative to the DMSO treated control is plotted ± SE (n=3).

D. PATU8988S cells were cultured in the presence of BSA, EGF, HRG or IGF1 (100 ng/ml) with 10% FBS and treated with a range of concentrations of BYL719. Cell proliferation was quantified after 72 h using CellTiter-Blue. The mean GI_{50} is plotted ± SE (n=6) and statistical significance compared to the BSA control was determined by one-way ANOVA.

E. PATU8988S cells were cultured in the presence of BSA, EGF, HRG or IGF1 (100 ng/ml) with 10% FBS and treated with DMSO (0.1 %) or BYL719 (2 μM) for 72 h. Cell lysates were analyzed by Western blotting (n=3).

Figure 3. A combinatorial drug screen identifies mTOR and ERBB-family inhibitors as potent enhancers of PI3K inhibition.

A. MIAPACA2 cells were treated with a library of 487 FDA-approved drugs and tool compounds at a concentration of 800 nM in the presence or absence of 10 µM BYL719 or 1 µM GDC0941. After 96 h, cell proliferation was quantified by CellTiter-Blue assay. Proliferation was normalized to a DMSO-treated control on each plate and the Bliss independence model was used to calculate synergy with BYL719 or GDC0941 for each of the compounds in triplicate. The mean Bliss score for each compound in combination with BYL719 was plotted against the mean Bliss score for each compound in combination with GDC0941.

B. The mean Bliss score for each compound in combination with BYL719 and GDC0941 was calculated and used to rank compounds. The top 20 compounds are shown.

C. Cells were incubated with a matrix of increasing concentrations of BYL719 and either pelitinib or AZD2014 for 144 h. Cell viability was measured using CellTiter-Blue and normalized to DMSO-treated wells (a shift from blue to red indicates loss of proliferation). The Bliss independence model was used to calculate synergy where a shift from green to red indicates increasing synergy (n=3).

D. Cells were incubated with the indicated compounds or the combinations in triplicate for 14 d. Cells were fixed and stained with 0.5 % crystal violet.

E. Spheroids consisting of a co-culture of MIAPACA2 cells and PSCs (1:1) were allowed to establish for 24 h and were then treated with the indicated compounds or the combination for 9 d. Dual calcein AM (viable cells) and propidium iodide (non-viable cells) staining was performed. Images were obtained using the Celigo imaging cytometer.

F. The diameter of the spheroid was measured every 3-4 d by quantification of images recorded on the Celigo. Colony diameter is plotted as the mean of at least three independent spheroids ± SE (n=2). Statistical significance was determined by one-way ANOVA with Tukey's multiple comparisons test.

G. Propidium iodide staining of spheroids was performed after 4 d and fluorescence intensity of the spheroid was quantified on the Celigo (n=6). Mean fluorescence intensity is represented by the horizontal bar. Statistical significance was determined by one-way ANOVA with Tukey's multiple comparisons test.

Figure 4. Inhibition of S6 phosphorylation is associated with synergistic, antiproliferative effects of combined PI3K and mTOR or pan-ERBB family inhibition.

A. MIAPACA2 and T47D cells were exposed to the indicated concentrations of BYL719 for 2 h or MIAPACA2_Cas9 cell clones lacking expression of p110α (knocked out via CRISPR-Cas9) were analysed by Western blotting for PI3K pathway activation using the indicated antibodies. NIC: no-infection control.

B. Percentage cell proliferation after incubation with 10 μM BYL719 for 72 h relative to DMSO (n=3) is plotted against percentage S6 phosphorylation, relative to DMSO, quantified from Western blots after incubation with 10 μM BYL719 for 2 h (n=2). Each point represents a different cell line from a panel of 12 PDAC cells. Linear regression analysis in GraphPad Prism was used to determine the correlation between the two variables.

C. MIAPACA2 cells were incubated with DMSO (0.1 %) BYL719 (10 μM), AZD2014 (250 nM), pelitinib (1 μM), or the indicated combinations for 72 h and cell lysates were analyzed by Western blotting (n=2).

Figure 5. Alterations in genes encoding the ERBB-family and selected downstream signalling mediators is associated with reduced pancreatic cancer patient survival.

A. Genetic alteration of the ERBB–PI3K signalling axis was assessed using cBioPortal and the TCGA 'provisional dataset' for 149 pancreatic cancer patients. 60 of 149 patients (40 %) displayed alterations in one or more of the indicated genes.

B. Overall survival of pancreatic cancer patients with or without genetic alterations of the genes shown in A. Significance was assessed by Log-rank Mantel-Cox test.

Author Manuscript Published OnlineFirst on May 5, 2020; DOI: 10.1158/1535-7163.MCT-19-1131
Author manuscripts have been peer reviewed and accepted for publication but have not yet been edited.

Figure 1. Milton *et al.*

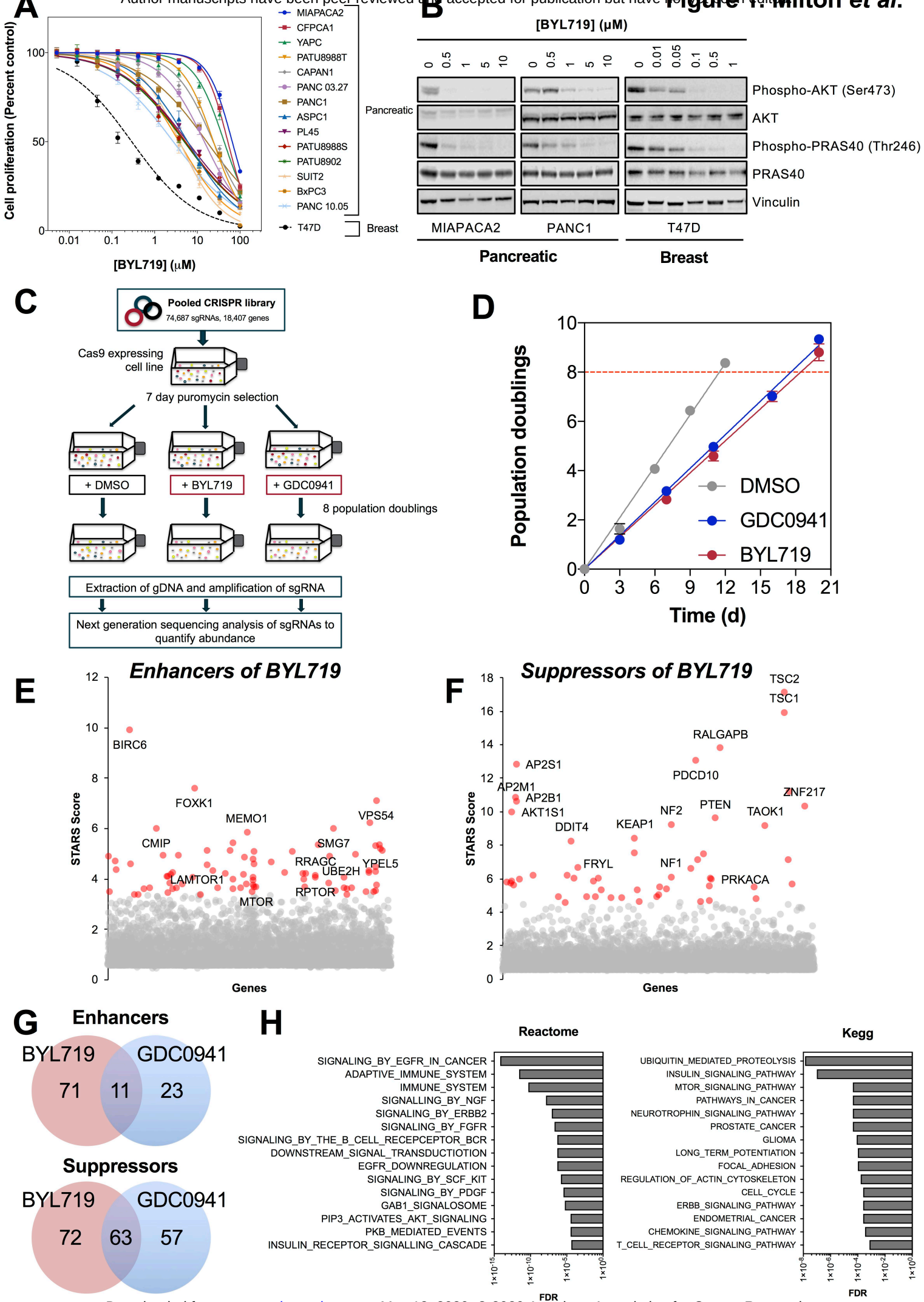

Figure 2. Milton *et al.*

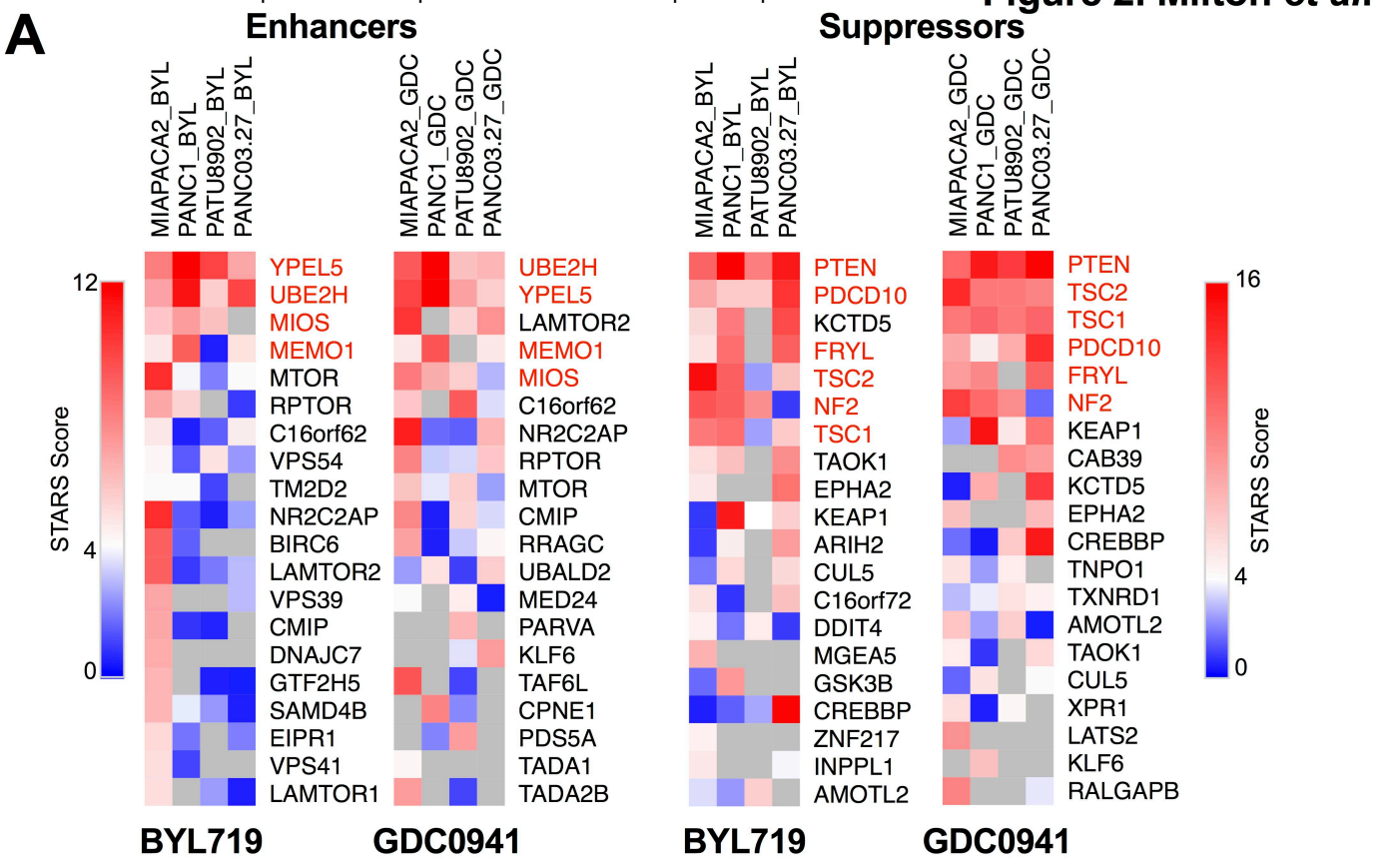

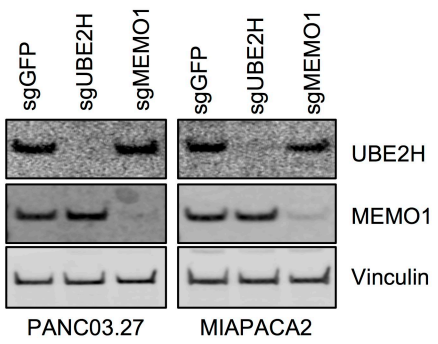

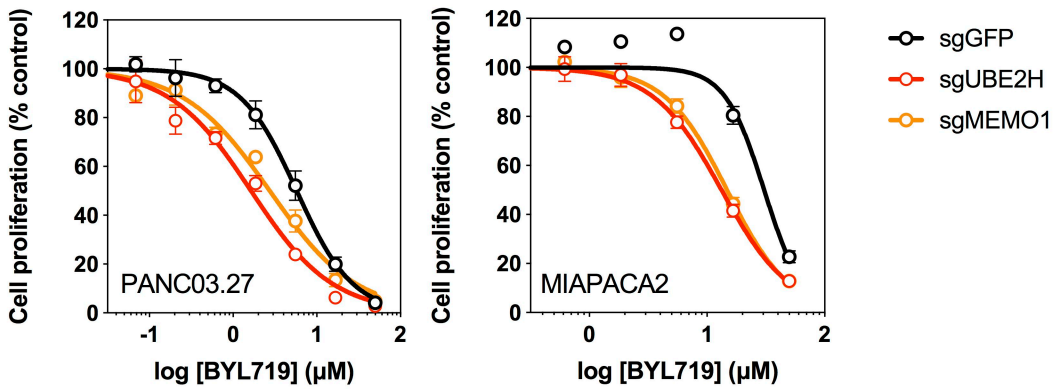

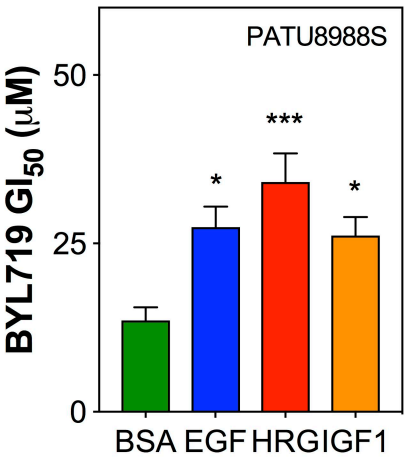

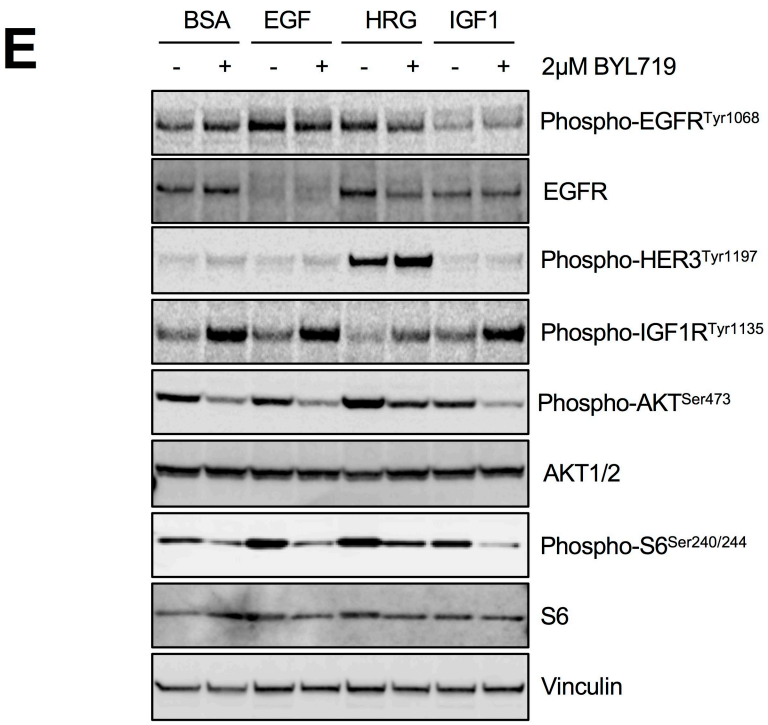

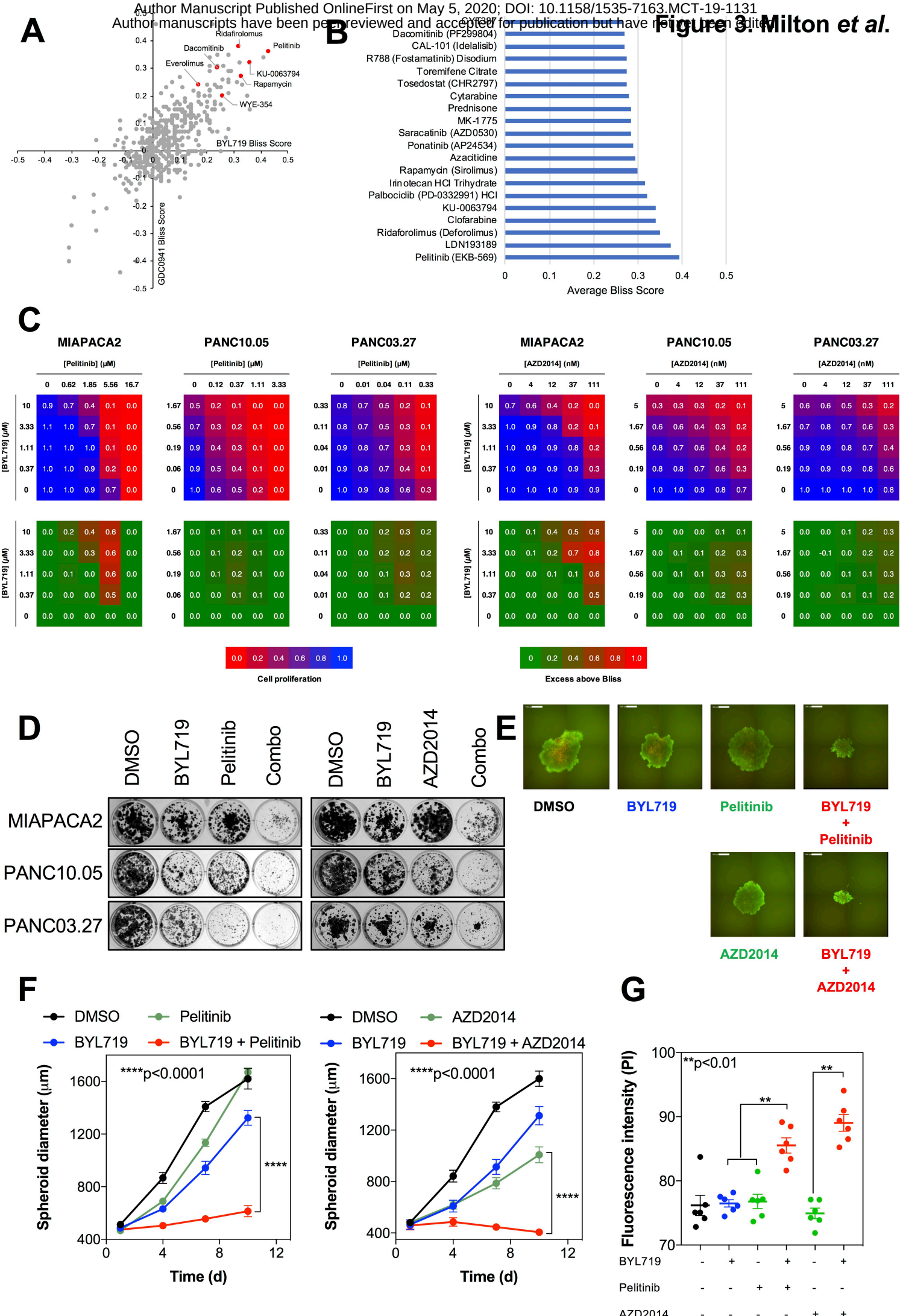

Author Manuscript Published OnlineFirst on May 5, 2020; DOI: 10.1158/1535-7163.MCT-19-1131

Figure 4. Milton *et al*.

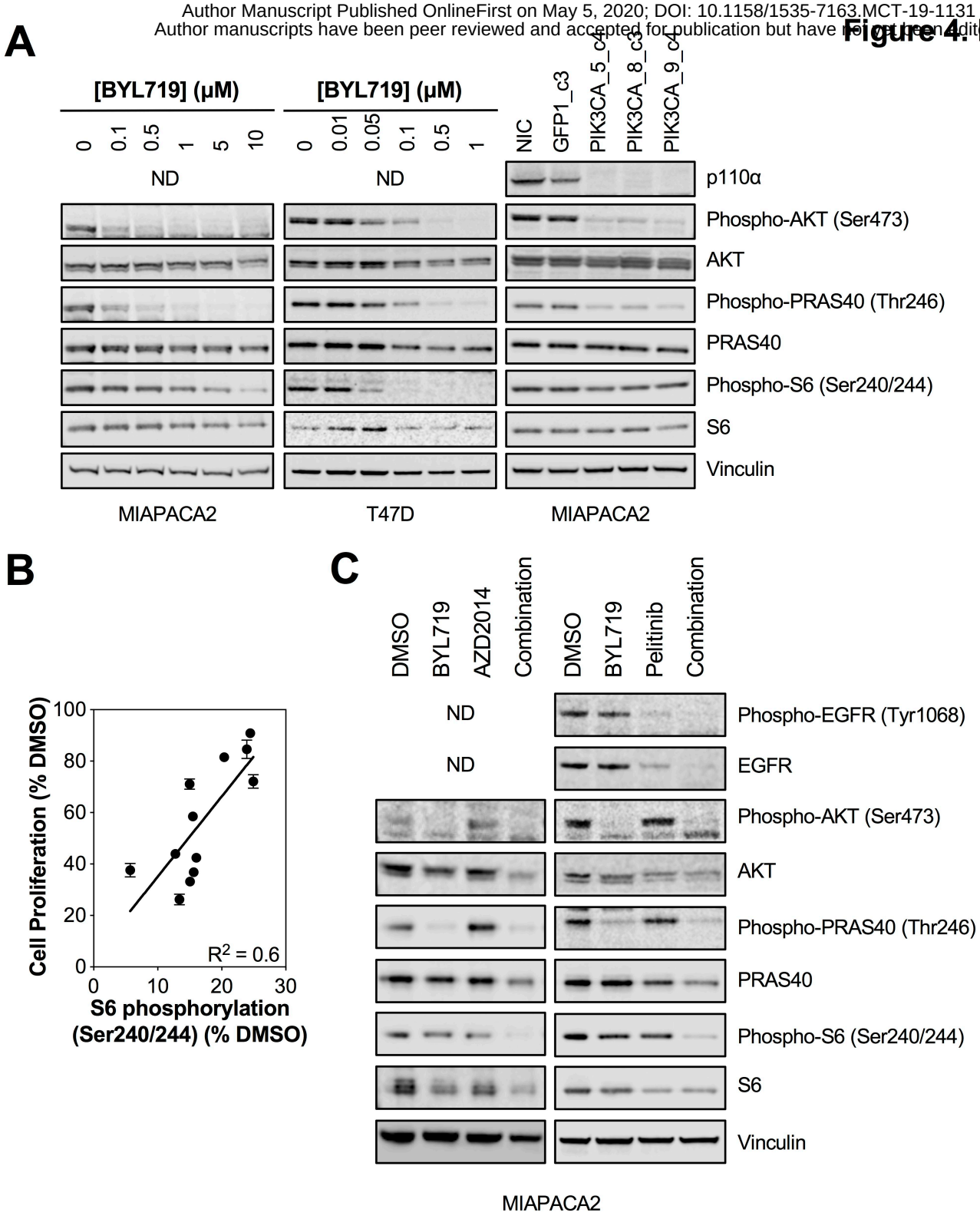

Author Manuscript Published OnlineFirst on May 5, 2020; DOI: 10.1158/1535-7163.MCT-19-1131

Figure 5. Milton *et al*.

AACR American Association for Cancer Research

Molecular Cancer Therapeutics

A genome-scale CRISPR screen identifies the ERBB and mTOR signalling networks as key determinants of response to PI3K inhibition in pancreatic cancer

Charlotte K Milton, Annette J Self, Paul A Clarke, et al.

Mol Cancer Ther Published OnlineFirst May 5, 2020.